

# Quantum tricritical point emerging in two dissipative spins in an antiferromagnetic bias field

Yan-Zhi Wang<sup>1</sup>, Shu He<sup>2</sup>, Liwei Duan<sup>1</sup>, and Qing-Hu Chen<sup>1,3,\*</sup>

<sup>1</sup> *Zhejiang Province Key Laboratory of Quantum Technology and Device,  
Department of Physics, Zhejiang University, Hangzhou 310027, China*

<sup>2</sup> *Department of Physics and Electronic Engineering,  
Sichuan Normal University, Chengdu 610066, China*

<sup>3</sup> *Collaborative Innovation Center of Advanced Microstructures, Nanjing University, Nanjing 210093, China*

(Dated: January 23, 2020)

We study the spin-boson model (SBM) with two spins in an antiferromagnetic bias field by a numerically exact method based on variational matrix product states. Several observables such as the magnetization, the entanglement entropy between the two spins and the bosonic environment, the ground-state energy, as well as the correlation function for two spins are calculated exactly. The characteristics of these observables suggest that the antiferromagnetic bias field can drive the 2nd-order quantum phase transition (QPT) to the 1st-order QPT in the sub-Ohmic SBM and the Kosterlitz-Thouless QPT directly to the 1st-order one in the Ohmic SBM. A quantum tricritical point, where the continuous QPT meets the 1st-order one, can be then detected. It is found that the antiferromagnetic bias field would not change the universality of this model below the quantum tricritical point.

PACS numbers: 03.65.Yz, 03.65.Ud, 71.27.+a, 71.38.k

## I. INTRODUCTION

Quantum phase transitions (QPTs) occur at zero temperature and are accompanied with a dramatic change in the physical properties of a systems near the critical parameters [1]. The same universality class can be shared by many different systems. It has been always the hot topics in the fields of solid-state systems and the light controlled condensed matter systems, such as the fermionic [2], spin [1], bosonic [3], as well as the fermion (spin)-boson coupling systems [4, 5]. Because fermions have both the spin and charge degree of freedom, so various quantum phases can emerge in the fermionic systems and bosonic ones if bosons are formed by composite fermions, such as fermion(boson)-Hubbard models in High-Tc superconductors and cold atoms. Among the light-matter interacting systems, it is well known for a long time that even the prototype Dicke model [6], and the spin-boson model (SBM) [7, 8] can display QPTs at strong coupling between the two-level systems (qubits) and the cavity or bosonic baths. Recently, it has been even proposed that the quantum Rabi model [9], which only includes one qubit and a single-mode cavity, can undergo a QPT in the infinite ratio of the qubit and cavity frequencies. It is generally accepted that the Dicke model and the quantum Rabi model only experience a single QPT from the normal to superradiant phase with the same critical behavior, and the SBM exhibits the single QPT from delocalized to localized phase with the power of the spectra function dependent criticality [10].

With the advance of modern technology in fabrication and bumping lights, the qubits and resonators (oscillators) coupling systems can be engineered in many solid-state devices, such as superconducting circuits [11], cold atoms in optical lattice [12], and trapped ions by tuned

and pulsed lights [13], which can be described by the prototype Dicke model and even its variants. More Recently, the SBM has been realized by the ultrastrong coupling of a superconducting flux qubit to an open one-dimensional (1D) transmission line [14]. Even deep-strong coupling between the qubits and resonates can be accessed experimentally [15], and the integration of many qubits can be also realized, such as the quantum supremacy using a programmable superconducting processor claimed by Google [16]. The rich and novel quantum phases might emerge in some generalized models.

Theoretically, to obtain rich phases in the light-matter interacting systems, one can generalize these prototype models. Generally, the QPT only appears in the Dicke model in the thermodynamic limit, i.e. the qubit number  $N \rightarrow \infty$ , exhibiting the mean-field critical behavior. The generalized Dicke models in the limit of  $N \rightarrow \infty$ , such as the anisotropic Dicke model [17, 18], the anisotropic Dicke model with the Stark coupling terms [19], and the Dicke model where infinite atoms are separated equally into two parts, each experiences an antiferromagnetic bias field [20] have been recently studied by several groups.

A quantum tricritical point (QuTP) [21] is seldomly supported in the solid-state materials, and is almost impossible to appear in the prototype models of the light-matter interacting systems. Interestingly, it has been found to exist in anisotropic Dicke model [18] and the isotropic Dicke model with antiferromagnetic bias fields [20]. In the former model, the QuTP lies at the symmetric line of the superradiant “electric” and “magnetic” phases which can be mapped mutually by interchanging the rotating-wave term and the counterrotating one. While in the latter model, it was demonstrated in Ref. [20] that the field can driven the 2nd QPTs in the Dicke

model to the 1st-order, thus 2nd-order critical line can meet 1st-order critical line at the QuTP.

In the original SBM with single qubit, the 2nd-order QPT from the delocalized phase, where spin has the equal probability in the two states, to localized phase, in which spin prefers to stay in one of the two states, has been studied extensively [10, 22–30]. It is generally accepted that the continuous QPT with mean-field exponents is found for the power of the spectral function of the bosonic baths  $s < 1/2$  [22, 23, 25], with nontrivial power for  $1/2 < s < 1$  [10, 24]. Kosterlitz-Thouless (KT) phase transition occurs for  $s = 1$  [5], and no phase transition happens for  $s > 1$ .

The SBM has been generalized by increasing the number of spins, such as the SBM with two spins [31, 32], and a number  $N$  of spins even in the limit  $N \rightarrow \infty$  [33]. It has been found that the critical behavior of QPT is not changed by the finite number of spins. In the limit  $N \rightarrow \infty$  the universality class of the transition changes to mean-field behavior, the same universality of the Dicke model. Motivated by the generalized Dicke model [20], we will study the criticality of the SBM with two spins in an antiferromagnetic bias field. Our goals are two-fold. One is whether such bias fields would change the universality class of the QPT. The other one is whether the bias fields result in the QuTP as the Dicke model.

In this paper, we will extend the variational matrix product state (VMPS) approach [27] to study the two-spin-boson model (2SBM) with the sub-Ohmic bath. The paper is organized as follows. In Sec. II, we introduce the 2SBM in the bias fields for two spins along the opposite directions and the VMPS approach briefly. In Sec. III, we study the QPTs of the 2SBM in sub-Ohmic and Ohmic bath with the antiferromagnetic bias field. For the sub-Ohmic bath, we choose two typical powers of the spectra function of the bath, which are, respectively, corresponding to the mean-field and non-mean-field critical nature of the QPTs in the single SBM. The order parameter and the entanglement entropy between the two qubits and the bosonic bath are extensively calculated. The critical exponents for the order parameter are also analyzed. A QuTP separated by the 2nd-order (KT type) critical lines and the 1st-order ones for the sub-Ohmic (Ohmic) baths are revealed by several independent evidences from different observables. Finally, we present the brief summary in the last section.

## II. 2SBM WITH AN ANTIFERROMAGNETIC BIAS FIELD AND METHODOLOGIES

The 2SBM Hamiltonian can be written as (the reduced Planck constant is set  $\hbar = 1$ )

$$\hat{H} = \sum_{i=1,2} \frac{1}{2} \left( \Delta \sigma_i^z - (-1)^i \epsilon \sigma_i^x \right) + \sum_k \omega_k a_k^\dagger a_k + \frac{1}{2} \sum_k g_k \left( a_k^\dagger + a_k \right) \left( \sigma_1^x + \sigma_2^x \right), \quad (1)$$

where  $\sigma_{i=1,2}^j$  ( $j = x, y, z$ ) are the Pauli matrices for spins 1 and 2,  $\Delta$  is the qubit frequency,  $(-1)^i \epsilon$  before  $\sigma_i^x$  is the bias field representing an antiferromagnetic bias field along the x axis for the two spins,  $a_k$  ( $a_k^\dagger$ ) is the bosonic annihilation (creation) operator which can annihilate (create) a boson with frequency  $\omega_k$ , and  $g_k$  denotes the coupling strength between the qubit and the bosonic bath, which is usually characterized by the power-law spectral density  $J(\omega)$ ,

$$J(\omega) = \pi \sum_k g_k^2 \delta(\omega - \omega_k) = 2\pi\alpha\omega_c^{1-s}\omega^s\Theta(\omega_c - \omega), \quad (2)$$

where  $\alpha$  is a dimensionless coupling constant,  $\omega_c$  is the cutoff frequency, and  $\Theta(\omega_c - \omega)$  is the Heaviside step function. The power of the spectral function  $s$  classifies the reservoir into super-Ohmic ( $s > 1$ ), Ohmic ( $s = 1$ ), and sub-Ohmic ( $s < 1$ ) types. This model is illustrated in Fig. 1 where the x-axis is in horizontal line.

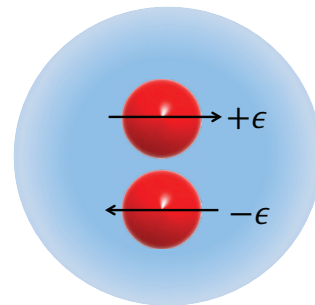


FIG. 1: (Color online) Illustration of the two-spin-boson model with the antiferromagnetic bias field  $\pm\epsilon$  along the x-direction. The two spins denoted by red spheres interact with a common continuous bosonic reservoir represented by the big blue region. No direct interaction between spins is considered.

The introduced antiferromagnetic bias fields to the two spins do not break the parity ( $Z_2$ ) symmetry in the 2SBM. Its parity operator is defined as

$$\hat{\Pi} = \left[ \frac{\sigma_1^z \sigma_2^z + 1}{2} - (\sigma_1^+ \sigma_2^- + \sigma_1^- \sigma_2^+) \right] \exp \left( i\pi \sum_k a_k^\dagger a_k \right), \quad (3)$$

where  $\sigma_{i=1,2}^\pm = (\sigma_i^x \pm i\sigma_i^y)/2$ . Note that in the presence of the bias field, it is more complicated than the parity for  $\epsilon = 0$ ,  $\hat{\Pi}_{\epsilon=0} = \exp \left[ i\pi \left( \sum_k a_k^\dagger a_k + (\sigma_1^z + \sigma_2^z)/2 + 1 \right) \right]$ , due to the absence of the collective spin. The parity operator  $\hat{\Pi}$  has two eigenvalues  $\pm 1$ , corresponding to even and odd parity in the symmetry conserved phases. The average value of the parity may become zero due to the quantum fluctuations in the symmetry broken phase.

To apply VMPS in the 2SBM in the antiferromagnetic bias fields, firstly the logarithmic discretization of the spectral density of the continuum bath [10] with discretization parameter  $\Lambda > 1$  is performed, followed by using orthogonal polynomials as described in Ref. [34], the

2SBM can be mapped into the representation of a one-dimensional semi-infinite chain with nearest-neighbor interaction [35]. Thus, Hamiltonian (1) can be written as:

$$H_{\text{chain}} = \frac{\Delta}{2} (\sigma_1^z + \sigma_2^z) + \frac{\epsilon}{2} (\sigma_1^x - \sigma_2^x) + \frac{c_0}{2} (b_0 + b_0^\dagger) (\sigma_1^x + \sigma_2^x) + \sum_{n=0}^{L-2} [\epsilon_n b_n^\dagger b_n + t_n (b_n^\dagger b_{n+1} + b_{n+1}^\dagger b_n)], \quad (4)$$

where  $b_n^\dagger (b_n)$  is the creation (annihilation) operator for a new set of boson modes in a transformed representation with  $\epsilon_n$  describing frequency on chain site  $n$ ,  $t_n$  describing the nearest-neighbor hopping parameter, and  $c_0$  describing the effective coupling strength between the spin and the new effective bath. For details, one may refer to Ref. [34].

Then as introduced in [36, 37], we employ the standard matrix product representation with optimized boson basis  $|\tilde{n}_k\rangle$  through an additional isometric map with truncation number  $d_{\text{opt}} \ll d_n$  like in Refs. [27, 35] to study the quantum criticality of 2SBM. Each site in the 1D chain can be described by the matrix  $M$ , which is optimized through sweeping the 1D chain iteratively to obtain the ground state, and  $D_n$  is the bond dimension for matrix  $M$  with the open boundary condition, bounding the maximal entanglement in each subspace.

For the data presented below, we typically choose the same model parameters in Ref. [27, 38, 39], as  $\Delta = 0.1$ ,  $\omega_c = 1$ , the logarithmic discretization parameter  $\Lambda = 2$ , the length of the semi-infinite chain  $L = 50$ , and optimized truncation numbers  $d_{\text{opt}} = 12$ . In addition, we adjust the bond dimension as  $D_{\text{max}} = 20, 40$ , and 20 for  $s = 0.3, 0.7$ , and 1, respectively, which are sufficient to obtain the converged results for the problems concerned.

The information of the ground-state can be also described by the Von Neumann entropy  $S_E$  of the 2SBM, which characterizes the entanglement between two spins and the bosonic bath

$$S_E = -\text{Tr}(\rho_{\text{spin}} \log \rho_{\text{spin}}), \quad (5)$$

where  $\rho_{\text{spin}}$  is the reduced density matrix for the two spins.

The averaged total magnetization

$$M = (\langle \sigma_1^x \rangle + \langle \sigma_2^x \rangle) / 2, \quad (6)$$

can be regarded as the order parameter, which can be used to characterize the essential nature of the 2nd-order QPTs. However, it is hardly employed to distinguish the KT and the 1st-order QPTs because both would suddenly drop to zero.

### III. RESULTS AND DISCUSSIONS

#### A. Sub-Ohmic bath ( $s < 1$ )

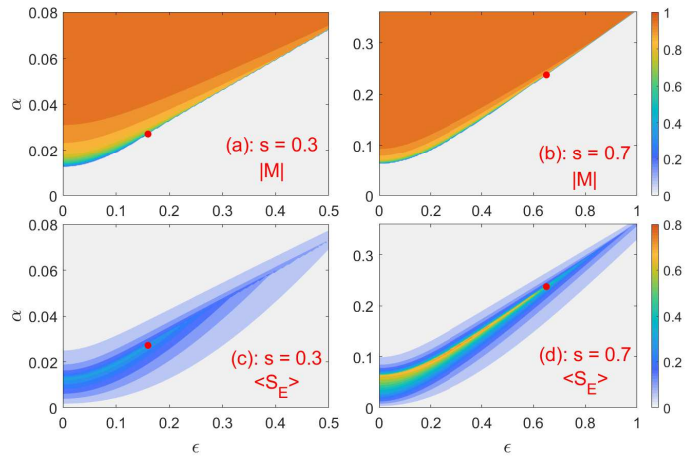


FIG. 2: (Color online) (upper panel) Phase diagram in the  $\epsilon - \alpha$  plane for 2SBM drawn from the Magnetization  $|M|$ : delocalized phases ( $M = 0$ ) and the localized phase ( $M \neq 0$ ). (lower panel) Entanglement entropy  $\langle S_E \rangle$ . The power of the spectral function is (left)  $s = 0.3$  and (right) 0.7.  $\Delta = 0.1$ ,  $\omega_c = 1$ . The QuTP is marked by a red dot, which separates the intersection of the 2nd- and 1st-order phase transition. The parameter used in the VMPS approach are  $\Lambda = 2$ ,  $L = 50$ ,  $d_{\text{opt}} = 12$ , and  $D = 20$  for  $s = 0.3, 0.7$ .

The single SBM expects a mean-field critical behavior for  $s < 1/2$ , and a nonclassical one for  $s > 1/2$ , so we focus on two typical powers of the spectral function  $s = 0.7$  and 0.3 in this work. The phase diagram of 2SBM in the opposite bias fields based on the VMPS approaches are presented in the  $\epsilon - \alpha$  plane of the upper panel in Fig. 2 for  $s = 0.3$  (left) and 0.7 (right). The entire critical lines can be mapped out by the boundary of the nonzero order parameter  $M = (\langle \sigma_1^x \rangle + \langle \sigma_2^x \rangle) / 2$ , which separates the delocalized phase and localized phase. Moreover, for the 2nd-order QPT, the order parameter becomes nonzero continuously, while in the 1st-order QPT, it suddenly jumps to a finite value. By this criterion, we can evaluate the QuTP that splits the whole critical line into the 1st- and 2nd-order critical lines, as indicated in the upper panel in Fig. 2 with red dots.

We also display the entanglement entropy between the two spin and the bath in the lower panel of Fig. 2. The ridge line is the critical line, because the highest entropy signifies the phase transitions [40]. The highly entanglement is observed near the whole critical line in both sides, and fall off fast away from the critical lines.

To study the QPTs deeply, we will discuss the order parameter and the entanglement entropy in detail. For more clear, we extract the data of the magnetization and the entropy as a function of coupling strength  $\alpha$  along  $\epsilon = 0.1$  and 0.2 for  $s = 0.3$ , along  $\epsilon = 0.5$  and 0.7 for

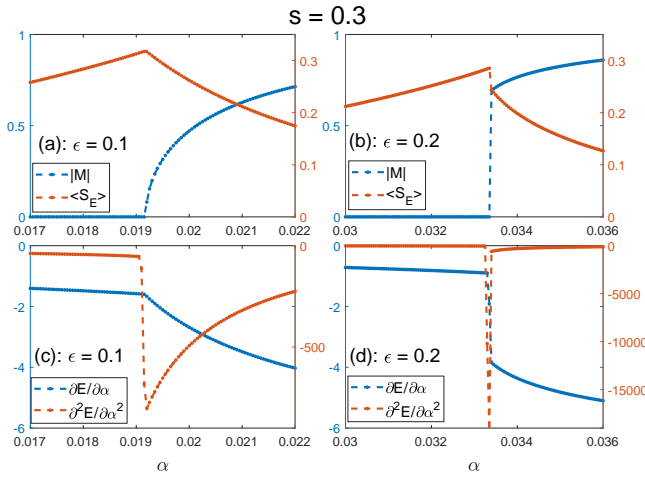


FIG. 3: (Color online) Magnetization  $|M|$ , Entanglement entropy  $\langle S_E \rangle$  (upper panels), and the first, second derivative of energy  $\partial E / \partial \alpha$ ,  $\partial^2 E / \partial \alpha^2$  (lower panels) as a function of  $\alpha$  in the ground state for  $\epsilon = 0.1$  (left) and  $\epsilon = 0.2$  (right) by VMPS approach.  $\Delta = 0.1$ ,  $\omega_c = 1$ ,  $\Lambda = 2$ ,  $L = 50$ ,  $d_{opt} = 12$ , and  $D = 20$  for  $s = 0.3$ .

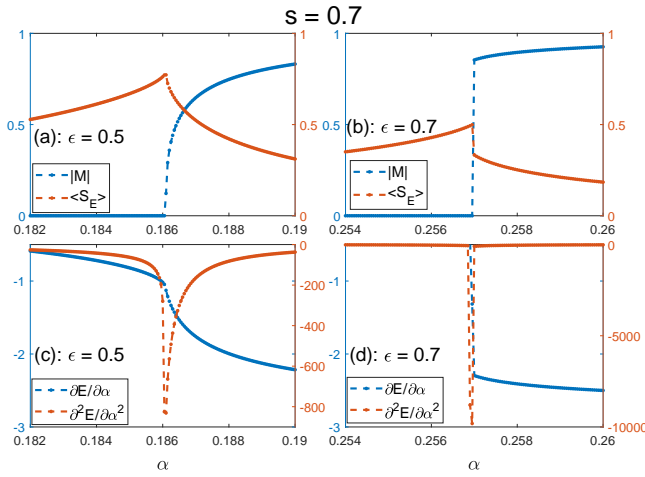


FIG. 4: (Color online) Magnetization  $|M|$ , Entanglement entropy  $\langle S_E \rangle$  (upper panels), and the first, second derivative of energy  $\partial E / \partial \alpha$ ,  $\partial^2 E / \partial \alpha^2$  (lower panels) as a function of  $\alpha$  in the ground state for  $\epsilon = 0.5$  (left) and  $\epsilon = 0.7$  (right) by VMPS approach.  $\Delta = 0.1$ ,  $\omega_c = 1$ ,  $\Lambda = 2$ ,  $L = 50$ ,  $d_{opt} = 12$ , and  $D = 20$  for  $s = 0.7$ .

at  $s = 0.7$ , and replot in the upper panel of Figs. 3 and 4, respectively. Here the two values of bias field in both powers of the spectra function of the baths are corresponding to the 2nd- and 1st-order QPTs. One can obviously find that the order parameter  $M$  becomes nonzero and cusps of the entropy appear right at the phase transition. Obviously, both  $M$  and  $S$  change continuously in the 2nd-order QPTs (upper left), but discontinuously in the 1st-order QPTs (upper right).

The 1st-order and 2nd-order QPTs can be also directly discerned by its first- and second-order derivative

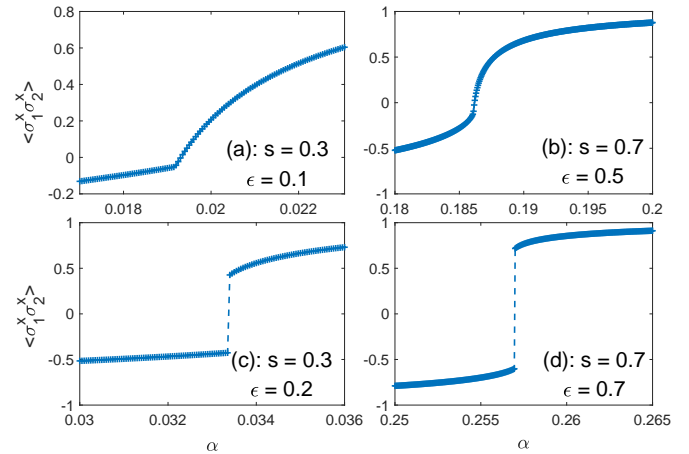


FIG. 5: (Color online) The correlation function  $\langle \sigma_1^x \sigma_2^x \rangle$  as a function of the coupling strength within VMPS approaches at  $\epsilon = 0.1, 0.2$  for  $s = 0.3$  (left) and  $\epsilon = 0.5, 0.7$  for  $s = 0.7$  (right). Other parameters:  $\Delta = 0.1$ ,  $\omega_c = 1$ ,  $\Lambda = 2$ ,  $L = 50$ ,  $d_{opt} = 12$ ,  $D = 20$ .

of the ground-state energy with respect to the coupling parameter  $\alpha$ . The results for the same parameters as in the upper panel of Figs. 3 and 4 are presented in the lower panels of the same figures. At the two smaller bias fields (lower left), the 1st-order derivatives of the energy are continuous around the transitions, while at the two larger bias fields (lower right), they are discontinuous at the critical points. The 2nd-order derivatives of the energy are discontinuous and diverge at the critical points for the smaller and larger  $\epsilon$ 's, respectively. The observation is in accord with the nature of the 2nd- and 1st-order phase transitions, justifying the existence of QuTP in the phase diagram based on the order parameter.

To provide further evidence of the existence of the QuTP separating the 1st- and 2nd-order critical lines, we calculate the two spin correlation function  $\langle \sigma_1^x \sigma_2^x \rangle$ . The results are shown in Fig. 5 for  $s = 0.3$  (left) and  $0.7$  (right), at small and large  $\epsilon$ 's, which are the same as those in Figs. 3 and 4. It is observed that the  $\langle \sigma_1^x \sigma_2^x \rangle$  is continuous (discontinuous) for small (large) bias fields  $\epsilon$ 's, also demonstrating the 2nd (1st)-order QPTs at small (large)  $\epsilon$ 's.

Since the antiferromagnetic bias field can drive the 2nd-order QPTs to the 1st-order ones, can it alter the universality class in the 2nd-order critical lines? In order to answer this question, we present the log-log plot of the magnetization  $M = (\langle \sigma_1^x \rangle + \langle \sigma_2^x \rangle) / 2$  as a function of  $\alpha - \alpha_c$  in Fig. 6 where the parameters are the same as those in Fig. 5. The critical exponents  $\beta$  can be determined by fitting power-law behavior,  $M \propto (\alpha - \alpha_c)^\beta$ . For two smaller  $\epsilon$ 's below the QuTP, as displayed in the upper panel of Fig. 6, very nice power-law behavior over three decades are demonstrated for both cases, yielding  $\beta = 0.484$  for  $s = 0.3$  and  $\beta = 0.303$  for  $s = 0.7$ , which are very close to those in the single SBM for the same  $s$



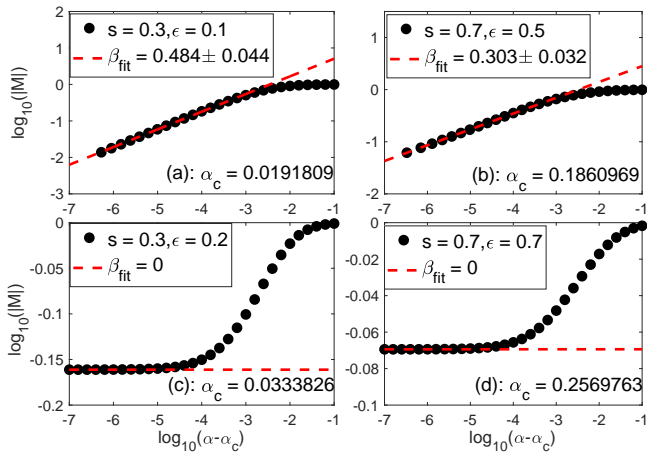


FIG. 6: (Color online) The log-log plot of the magnetization  $|M|$  as a function of  $\alpha - \alpha_c$  at  $\epsilon = 0.1, 0.2$  for  $s = 0.3$  (left) and  $\epsilon = 0.5, 0.7$  for  $s = 0.7$  (right). The numerical results by VMPS are denoted by black circles and the power-law fitting curves are denoted by the red dashed lines, which indicates the 2nd-order QPT takes place in the smaller bias field and gives similar critical behaviors compared to the standard spin-boson model, while the larger bias field induces the 1st-order QPT and vanishing of the critical exponent  $\beta$ .  $\Delta = 0.1, \omega_c = 1, \Lambda = 2, L = 50, d_{opt} = 12$ , and  $D = 20, 40$  for  $s = 0.3, 0.7$  respectively.

by the VMPS approaches [27]. This is to say, the critical exponents of the order parameter are not different from those in the single SBM. In other words, as long as the 2nd-order QPTs occurs in the 2SBM with the antiferromagnetic bias field, the critical exponent is only the bath exponent dependent, and remains unchanged with  $\epsilon$ . At the 1st-order critical line which is in the larger  $\epsilon$  region, as shown in the low panel of Fig. 6,  $\beta = 0$ , which is in accord with the 1st-order phase transition nature.

### B. Ohmic bath ( $s=1$ )

It is well known that the single SBM with the Ohmic bath undergoes the continuous QPTs of KT type [5]. In the language of the quantum-to-classical mapping,  $s = 1$  corresponds to the low critical dimension of the long-ranged Ising model [41]. Recall in the last section, the antiferromagnetic bias field can drive the 2nd-order QPTs to the 1st-order one in the sub-Ohmic 2SBM. Note that the finite number of spins would not change the universality of the SBM [33]. What is the effect of these bias fields on the KT phase transitions in the Ohmic 2SBM? Could the bias field drive the KT phase transitions to the 2nd-order or/and the 1st-order ones?

To address these issues, we perform the VMPS study on 2SBM in the Ohmic bath with the bias fields described above. In the literature, the entanglement entropy is usually checked in the SBM with the Ohmic bath, because

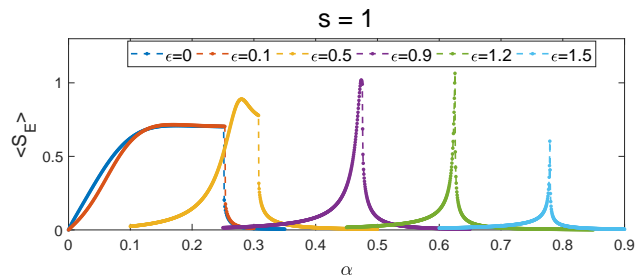


FIG. 7: (Color online) Entanglement entropy  $\langle S_E \rangle$  as a function of  $\alpha$  in the ground state at  $\epsilon = 0, 0.1, 0.5, 0.9, 1.2, 1.5$  for  $s = 1$  by VMPS approach.  $\Delta = 0.1, \omega_c = 1, \Lambda = 2, L = 50, d_{opt} = 12$ , and  $D = 20$ .

KT phase transitions are of infinite order, and less observables can be used to distinguish KT from other kinds of phase transitions. In the KT phase transition of the single SBM for the bath exponent  $s = 1$ , the entropy increases in the weak coupling regime, then saturates to a plateau, and drops suddenly at the KT critical point [42]. In the 2nd-order QPTs, the entropy falls off both sides of the critical point [26].

We calculate the entropy for several bias fields from  $\epsilon = 0$  to 1.5 in Fig. 7. We find that after the plateau, all entropies suddenly drop at the transition point. With the increase of the field, the flat plateaus gradually change into the broad peak, and shrink considerably if we further go to larger  $\epsilon$ , such as  $\epsilon = 0.9$  where the peak point is very close to but not at the transition point. We believe that as long as the peak point does not meet the transition point, it is still in the universality of the KT phase transitions. It is interesting to note that for  $\epsilon = 0.5, 0.99$ , the entropy shows a broad peak before drops abruptly at the localized transition, different from that in the single SBM for  $s = 1$ . One may argue that coherence is lost already before the system becomes localized [31].

Next, to demonstrate the bias field driven new phase transitions in the 2SBM in the larger  $\epsilon$ , we present the entropy for smaller fields in Fig. 8, and larger fields in Fig. 9. The order parameter jumps suddenly for all cases at the transitions, so one could not employ it to discriminate between the 1st-order and the KT type of QPTs. The entropy drops abruptly at the transition points for all bias fields. However, for small bias fields shown in Fig. 8, it decreases with  $\alpha$  before the abrupt drop, contrary to the case for large fields indicated in Fig. 9 where a cusp of the entropy appears the transition points (lower panel), i.e. the entropy falls off in both sides. The different behaviors are originated from different kinds of phase transitions.

To show the nature of the phase transition more directly, we also display the corresponding first-order and second-order derivatives of the ground-state energy with respect to  $\alpha$ . It is found in Fig. 8 that for small field, at the transition point, both  $\partial E / \partial \alpha$  and  $\partial^2 E / \partial \alpha^2$  are continuous and have no exotic behavior. Even the further

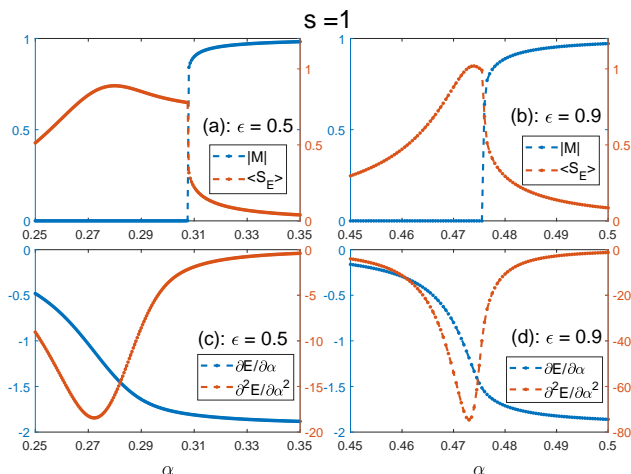


FIG. 8: (Color online) Magnetization  $|M|$ , Entanglement entropy  $\langle S_E \rangle$  (upper panels), and the first, second derivative of energy  $\partial E/\partial\alpha$ ,  $\partial^2 E/\partial\alpha^2$  (lower panels) as a function of  $\alpha$  in the ground state for  $\epsilon = 0.5$  (left) and  $\epsilon = 0.9$  (right) by VMPS approach.  $\Delta = 0.1$ ,  $\omega_c = 1$ ,  $\Lambda = 2$ ,  $L = 50$ ,  $d_{opt} = 12$ , and  $D = 20$  for  $s = 1$ .

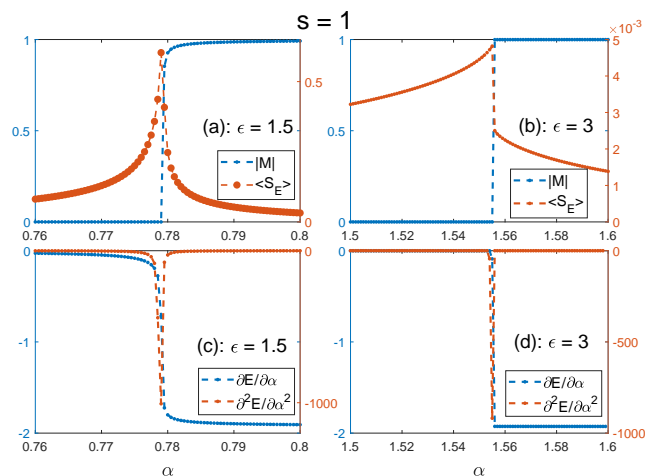


FIG. 9: (Color online) Magnetization  $|M|$ , Entanglement entropy  $\langle S_E \rangle$  (upper panels), and the first, second derivative of energy  $\partial E/\partial\alpha$ ,  $\partial^2 E/\partial\alpha^2$  (lower panels) as a function of  $\alpha$  in the ground state for  $\epsilon = 1.5$  (left) and  $\epsilon = 3$  (right) by VMPS approach.  $\Delta = 0.1$ ,  $\omega_c = 1$ ,  $\Lambda = 2$ ,  $L = 50$ ,  $d_{opt} = 12$ , and  $D = 20$  for  $s = 1$ .

high order derivative would not exhibit any discontinuity at this point due to the infinite-order KT phase transition nature.

However, as shown in Fig. 9 for two larger bias fields,  $\partial E/\partial\alpha$  drops suddenly and  $\partial^2 E/\partial\alpha^2$  diverges at the

transition point for all cases. This is typical characteristics of the 1st-order phase transitions. We have carefully checked many large bias fields, we have not found any signature of the 2nd-order phase transitions. Together with the observations in sub-Ohmic case in the last subsection, we can reach a conclusion that the antiferromagnetic bias field could not change the universality of continuous phase transitions including the KT ones in the 2SBM. We believe that this conclusion can be generalized to the finite even number dissipative spins in the antiferromagnetic bias field.

The universality in the QuTP in the present model is also a challenging issue. According to the Landau theory, it should be different from those in other critical points. But it is difficult to use any numerical approaches to distinguish this isolated point from others. If the analytical treatment formulated from the Feynman path-integral representation of the partition function for the single SBM [5, 43–45] can be extended to this model, then it may be probable to clarify this issue.

#### IV. CONCLUSION

We have found rich quantum phases in the 2SBM with both sub-Ohmic and Ohmic baths in the antiferromagnetic bias field by the VMPS approach. The phase diagram has been composed in the coupling strength and the bias fields. For sub-Ohmic bath, we really find that the 2nd-order critical lines meet the first-order ones at the QuTP with the bias field. For Ohmic bath, we find that the bias field will drive the KT phase transitions directly to the 1st-order phase transitions. For all case, if the 1st-order phase transition does not emerge, the universality of the phase transition could not be changed by the external antiferromagnetic bias field.

Since the recent superconducting circuit QED system allows for the SBM in an Ohmic bath [14], the 2SBM might be realized in any kinds of bath spectra in the near future. The bias field can be easily introduced to the artificial two-level systems by an externally applied magnetic flux, so the antiferromagnetic bias field is not difficult to manipulate. We believe that the 2SBM would become potential platform to test the rich quantum criticality and the QuTP.

**ACKNOWLEDGEMENTS** This work is supported by the National Science Foundation of China (Nos. 11834005, 11674285), the National Key Research and Development Program of China (No. 2017YFA0303002),

\* Email:qhchen@zju.edu.cn

[1] S. Sachdev, *Quantum Phase Transitions*, 2nd ed. (Cambridge University Press, Cambridge, England, 2011).

[2] V. J. Emery in *Highly Conducting One-Dimensional Solids*, edited by J.T. Devreese et al. (Plenum, New

- York, 1979), pp. 247–303; J. Solyom, *Adv. Phys.* **28**, 201 (1979); H.-Q. Lin et al., in *The Hubbard Model: Its Physics and Mathematical Physics*, edited by D. Baeriswyl, pp. 315–327.
- [3] M. Greiner, O. Mandel, T. Esslinger, T. W. Haensch, and I. Bloch, *Nature(London)* **415**, 39 (2002).
- [4] E. Fradkin and J. E. Hirsch, *Phys. Rev. B* **27**, 1680 (1983); W.-Q. Ning, H. Zhao, C.-Q. Wu, and H.-Q. Lin, *Phys. Rev. Lett.* **96**, 156402 (2006); E. A. Nowadnick, S. Johnston, B. Moritz, R. T. Scalettar, and T. P. Devereaux, *Phys. Rev. Lett.* **109**, 246404 (2012).
- [5] A. J. Leggett, S. Chakravarty, A. T. Dorsey, M. P. A. Fisher, A. Garg, and W. Zwerger, *Rev. Mod. Phys.* **59**, 1(1987).
- [6] R. H. Dicke, *Phys. Rev.* **93**, 99 (1954); C. Emary and T. Brandes, *Phys. Rev. E* **67**, 066203 (2003); *Phys. Rev. Lett.* **90**, 044101 (2003); Q.-H. Chen, Y.-Y. Zhang, T. Liu, and K.-L. Wang, *Phys. Rev. A* **78**, 051801 R (2008); T. Liu, Y.-Y. Zhang, Q.-H. Chen, and K.-L. Wang, *Phys. Rev. A* **80**, 023810(2009).
- [7] H. P. Breuer and F. Petruccione, *The Theory of Open Quantum Systems* (Oxford University Press, New York, 2002).
- [8] U. Weiss, *Quantum Dissipative Systems* (World Scientific Publishing Company, 2008).
- [9] M.-J. Hwang, R. Puebla, and M. B. Plenio, *Phys. Rev. Lett.* **115**, 180404 (2015); M. X. Liu, S. Chesi, Z.-J. Ying, X. S. Chen, H.-G. Luo, H.-Q. Lin, *Phys. Rev. Lett.* **119**, 220601 (2017).
- [10] R. Bulla, N. Tong, and M. Vojta, *Phys. Rev. Lett.* **91**, 170601 (2003); M. Vojta, N. Tong, and R. Bulla, *Phys. Rev. Lett.* **94**, 070604 (2005); R. Bulla, *Phys. Rev. Lett.* **102**, 249904(E) (2009).
- [11] T. Niemczyk et al., *Nature Physics* **6**, 772 (2010).
- [12] F. Dimer, B. Estienne, A. S. Parkins, and H. J. Carmichael, *Phys. Rev. A* **75**, 013804 (2007); K. Baumann, C. Guerlin, F. Brennecke, and T. Esslinger, *Nature (London)* **464**, 1301 (2010).
- [13] J. I. Cirac, A. S. Parkins, R. Blatt, and P. Zoller, *Phys. Rev. Lett.* **70**, 556 (1993).
- [14] P. Forn-Díaz, J. J. García-Ripoll, B. Peropadre, J.-L. Orgiazzi, M. A. Yurtalan, R. Belyansky, C. M. Wilson, and A. Lupascu, *Nat. Phys.* **13**, 39 (2017).
- [15] F. Yoshihara, T. Fuse, S. Ashhab, K. Kakuyanagi, S. Saito, and K. Semba, *Nat. Phys.* **13**, 44 (2017).
- [16] F. Arute et al., *Nature* **574**, 505(2019).
- [17] J. Ye and C. L. Zhang, *Phys. Rev. A* **84**, 023840 (2011).
- [18] A. Baksic and C. Ciuti, *Phys. Rev. Lett.* **112**, 173601 (2014).
- [19] Z. Q. Zhang, C. H. Lee, R. Kumar, K. J. Arnold, S. J. Masson, A. L. Grimsmo, A. S. Parkins, and M. D. Barrett, *Phys. Rev. A* **97** 043858 (2018).
- [20] Y. Xu and H. Pu, *Phys. Rev. Lett.* **122**, 193201 (2019).
- [21] R. B. Griffiths, *Phys. Rev. Lett.* **24**, 715 (1970).
- [22] A. Winter, H. Rieger, M. Vojta, and R. Bulla, *Phys. Rev. Lett.* **102**, 030601 (2009).
- [23] A. Alvermann and H. Fehske, *Phys. Rev. Lett.* **102**, 150601 (2009).
- [24] M. Vojta, R. Bulla, F. Güttge, and F. Anders, *Phys. Rev. B* **81**, 075122 (2010).
- [25] Y.-Y. Zhang, Q.-H. Chen, and K.-L. Wang, *Phys. Rev. B* **81**, 121105(R)(2010).
- [26] A. W. Chin, J. Prior, S. F. Huelga and M. B. Plenio, *Phys. Rev. Lett.* **107**, 160601 (2011).
- [27] C. Guo, A. Weichselbaum, J. von Delft, and M. Vojta, *Phys. Rev. Lett.* **108**, 160401 (2012).
- [28] M. F. Frenzel and M. B. Plenio, *New Journal of Physics* **15**, 073046(2013).
- [29] C. R. Duan, Z. F. Tang, J. S. Cao, and J. L. Wu, *Phys. Rev. B* **95**, 214308 (2017).
- [30] S. He, Li. W. Duan, and Q. -H. Chen, *Phys. Rev. B* **97**, 115157 (2018).
- [31] P. P. Orth, D. Roosen, W. Hofstetter, and K. Le Hur, *Phys. Rev. B* **82**, 144423 (2010).
- [32] H. Zheng, Z. G. Lu, and Y. Zhao, *Phys. Rev. E* **91**, 062115 (2015).
- [33] A. Winter and H. Rieger, *Phys. Rev. B* **90**, 224401 (2014).
- [34] A. W. Chin, A. Rivas, S. F. Huelga, and M. B. Plenio, *Journal of Mathematical Physics* **51**, 092109 (2010).
- [35] F. A. Y. N. Schröder, A. W. Chin, *Phys. Rev. B* **93**, 075105 (2016).
- [36] A. Weichselbaum, F. Verstraete, U. Schollwöck, J. I. Cirac, and J. von Delft, *Phys. Rev. B* **80**, 165117 (2009).
- [37] H. Saberi, A. Weichselbaum, and J. von Delft, *Phys. Rev. B* **78**, 035124 (2008).
- [38] Y.-Z. Wang, S He, L.-W. Duan, Q.-H. Chen. *Phys. Rev. B* **100**, 115106 (2019).
- [39] Y.-Z. Wang, S He, L.-W. Duan, Q.-H. Chen. arXiv:2001.02166.
- [40] K. Le Hur, P. Doucet-Beaupre and W. Hofstetter, *Phys. Rev. Lett.* **99**, 126801 (2007).
- [41] M. E. Fisher, *Phys. Rev. Lett.* **29**, 917 (1972); E. Luijten and Henk Blöte, *Phys. Rev. B* **56**, 8945 (1997).
- [42] A. Kopp and K. Le Hur, *Phys. Rev. Lett.* **98**, 220401 (2007).
- [43] M. Vojta, *Phys. Rev. B* **85**, 115113 (2012)
- [44] S. Kirchner, *J. Low Temp. Phys.* **161**, 282 (2010).
- [45] S. Kirchner, Q. Si, and K. Ingersent, *Phys. Rev. Lett.* **102**, 166405 (2009); S. Kirchner, K. Ingersent, and Q. Si, *Phys. Rev. B.* **85**, 075113(2012).